

## THE $Y_{SZ}-Y_X$ SCALING RELATION AS DETERMINED FROM *PLANCK* AND *CHANDRA*

EDUARDO ROZO<sup>1,2</sup>, ALEXEY VIKHLININ<sup>3,4</sup>, SURHUD MORE<sup>1</sup>

*Draft version June 28, 2018*

### ABSTRACT

SZ clusters surveys like *Planck*, the South Pole Telescope, and the Atacama Cosmology Telescope, will soon be publishing several hundred SZ-selected systems. The key ingredient required to transport the mass calibration from current X-ray selected cluster samples to these SZ systems is the  $Y_{SZ}-Y_X$  scaling relation. We constrain the amplitude, slope, and scatter of the  $Y_{SZ}-Y_X$  scaling relation using SZ data from *Planck* and X-ray data from *Chandra*. We find a best fit amplitude of  $\ln(D_A^2 Y_{SZ}/CY_X) = -0.202 \pm 0.024$  at the pivot point  $CY_X = 8 \times 10^{-5} \text{ Mpc}^2$ . This corresponds to a  $Y_{SZ}/Y_X$ -ratio of  $0.82 \pm 0.024$ , in good agreement with X-ray expectations after including the effects of gas clumping. The slope of the relation is  $\alpha = 0.916 \pm 0.032$ , consistent with unity at  $\approx 2.3\sigma$ . We are unable to detect intrinsic scatter, and find no evidence that the scaling relation depends on cluster dynamical state.

*Subject headings:* clusters

### 1. INTRODUCTION

The Sunyaev–Zeldovich effect — i.e. the prediction that the hot intra-cluster gas of massive galaxy clusters will scatter CMB photons to produce a unique frequency signature — traces back to 1972 (Sunyaev & Zeldovich 1972). Despite early detections of this effect (Gull & Northover 1976), it is only recently that instrumentation advances have made large scale SZ searches feasible. There are three such ongoing surveys: one carried out with the South Pole Telescope (SPT Carlstrom et al. 2011), one with the Atacama Cosmology Telescope (ACT Fowler et al. 2007), and one using the *Planck* satellite (Planck Collaboration 2011e). All three surveys have published initial cluster samples (Vanderlinde et al. 2010; Marriage et al. 2011; Planck Collaboration 2011d), and are expected to eventually publish hundreds of SZ selected systems out to  $z = 1$  and beyond. If the scaling relation between the integrated SZ signal and cluster mass can be adequately calibrated, then these cluster samples may be used to constrain the growth of large scale structure in the universe, which can in turn provide critical constraints on dark energy models (e.g. Holder et al. 2001). Indeed, both SPT and ACT have already derived cosmological constraints from their current samples (Vanderlinde et al. 2010; Sehgal et al. 2011; Benson et al. 2011).

Unfortunately, at this time no single method provides masses of individual clusters with a required  $\sim 5\%$  uncertainty. X-ray hydrostatic measurements are observationally expensive and limited to a subset of relaxed systems. Numerical simulations suggest that hydrostatic mass estimates can be biased low anywhere between 10% to 30% (Nagai et al. 2007; Piffaretti & Valdarnini 2008; Jeltama et al. 2008; Lau et al. 2009; Meneghetti et al.

2010; Rasia et al. 2012). Weak lensing estimates are in principle unbiased, but specific implementations can result in  $\approx 5\% - 10\%$  biases depending on the fitting procedure (typically biased high when using NFW fitting formulae Becker & Kravtsov 2010; Meneghetti et al. 2010; Rasia et al. 2012), and exhibit large intrinsic scatter. In addition, without the help from X-ray data, the derived SZ signal from the current generation surveys has a comparatively large scatter at a fixed mass (Benson et al. 2011; Planck Collaboration 2011d). Mass calibration using velocity dispersions is also possible (e.g. Evrard et al. 2008; Sifon et al. 2012), but subject to velocity bias. Therefore, the precise calibration of the cluster masses from SZ surveys will be possible only through a combined analysis of the SZ, X-ray, and optical data. Consequently, all three of the on-going SZ experiments are devoting significant effort for extensive X-ray and weak lensing follow-up of the SZ-selected systems (Andersson et al. 2010; Foley et al. 2011; Planck Collaboration 2011b,f; Menanteau et al. 2011).

Another possibility, however, is simply to transfer the existing calibration of the mass-proxy relations in the X-ray samples (e.g. Arnaud et al. 2007; Allen et al. 2008; Vikhlinin et al. 2009; Arnaud et al. 2010; Mantz et al. 2010) using the correlation of the cluster SZ parameters with the X-ray proxies (e.g. Benson et al. 2011). An important step in this process is to verify a tight correlation between the integrated SZ signal,  $Y_{SZ}$ , and its X-ray analog,  $Y_X = T_X \times M_{\text{gas},X}$  (Kravtsov et al. 2006, see section 1.1 for more precise definitions of  $Y_{SZ}$  and  $Y_X$ ). In addition to transferring the mass calibration, the  $Y_{SZ} - Y_X$  relation can be used to verify some key predictions of the structure formation theory which is used for applying the cosmological models to the cluster data. First, numerical simulations consistently show that both  $Y_{SZ}$  and  $Y_X$  have low scatter at a fixed mass ( $\approx 10\% - 15\%$ , Nagai 2006; Kravtsov et al. 2006; Stanek et al. 2010; Fabjan et al. 2011; Kay et al. 2011). Thus, we can expect the  $Y_{SZ}-Y_X$  relation to have very low scatter, especially since these parameters approxi-

<sup>1</sup> Kavli Institute for Cosmological Physics, Chicago, IL 60637, USA

<sup>2</sup> Department of Astronomy, University of Chicago, Chicago, IL 60637, USA

<sup>3</sup> Space Research Institute (IKI), Profsoyuznaya 84/32, Moscow 117810, Russia

<sup>4</sup> Harvard-Smithsonian Center for Astrophysics, 60 Garden St., Cambridge, MA 02138, USA

mate the same physical quantity, the thermal energy in the cluster gas. Second, these same simulations predict nearly self-similar evolution in the  $Y - M$  relation for both  $Y_X$  and  $Y_{SZ}$ , so we expect the  $Y_{SZ} - Y_X$  relation to have nearly the same normalization at both low and high redshifts.

The  $Y_{SZ} - Y_X$  relation has been reported in several recent works — by Andersson et al. (2010) at high- $z$  using SPT and *Chandra*, and at low- $z$  by Planck Collaboration (2011a) using Planck and *XMM-Newton*. The results are generally in line with the theoretical expectations —  $Y_{SZ}$  follows  $Y_X$  with a small overall offset. However, there are several issues which warrant further study. The overall offset between  $Y_X$  and  $Y_{SZ}$  is expected because real clusters are non-isothermal and slightly non-uniform. Given the overall  $\rho^2$  weighting of X-ray emission versus the  $\rho$  weighting of the SZ-signal, one naturally expects the two quantities to differ (see below for further details). Based on the analysis of *XMM-Newton* temperature profiles in a “representative” sample of clusters, Arnaud et al. (2010) predicted  $Y_{SZ}/Y_X = 0.924$ . The mean offset in the SPT/*Chandra* sample of Andersson et al. (2010) is somewhat below this prediction,  $Y_{SZ}/Y_X = 0.82 \pm 0.07$ . The mean offset in the Planck/*XMM-Newton* sample is  $1\sigma$  above,  $Y_{SZ}/Y_X = 0.95 \pm 0.03$  (Planck Collaboration 2011a). While the difference in the  $Y_{SZ}/Y_X$  ratio is relatively large, it is not significant because of the large errors in the Andersson et al. (2010) measurement, so additional measurements that reduce the statistical uncertainty of *Chandra* estimates of the  $Y_{SZ}/Y_X$  ratio are of great interest. This is particularly true in light of known differences in instrument calibration between *Chandra* and *XMM* so having a low-redshift calibration of this ratio using *Chandra* is of significant interest. Finally, the scatter in the *Planck/XMM*  $Y_{SZ} - Y_X$  relation is  $23\% \pm 2\%$ , which is significantly larger than the expected  $\approx 10\%$  scatter, so confirmation of this observation is important.

The goal of this paper is to measure the local  $Y_{SZ} - Y_X$  relation independently using overlapping clusters in the Planck and Vikhlinin et al. (2009) *Chandra* sample. This is the first step towards *Chandra*-based calibration of the local  $Y_{SZ} - M$  relation. We defer the actual calibration of the  $Y_{SZ} - M$  relation to an upcoming paper, where we simultaneously consider several the  $Y_{SZ} - M$  scaling relation as calibrated by several groups (Rozo et al. 2011). In this context, we emphasize that the *Chandra* X-ray results quoted here are derived from the gas temperature and gas density models for individual clusters taken from Vikhlinin et al. (2009). Consequently, this work and that of Vikhlinin et al. (2009) are fully self-consistent in all definitions.

Throughout this work, we assume a flat  $\Lambda$ CDM cosmology with  $\Omega_m = 0.3$  and  $h = 0.72$ . This convention matches that of Vikhlinin et al. (2009).

### 1.1. What We Mean by the $Y_{SZ}/Y_X$ Ratio

The  $Y_{SZ}$  signal of a galaxy cluster is related to the total pressure of the intra-cluster gas within the cluster’s volume via

$$D_A^2 Y_{SZ} = C \int dV \rho_{gas}(\mathbf{x}) T(\mathbf{x}) \quad (1)$$

where  $D_A$  is the angular diameter distance, and  $C$  is a constant that switches the units back and forth from  $M_\odot \text{keV}$  to  $\text{Mpc}^2$ . The constant  $C$  is given by

$$C = \frac{\sigma_T}{m_e c^2} \frac{1}{\rho_{gas}/n_e} = 1.406 \times \frac{10^{-5} \text{ Mpc}^2}{10^{14} \text{ keV} M_\odot}, \quad (2)$$

where  $\sigma_T$  is the Thompson cross-section, and  $\rho_{gas}/n_e = 1.149 m_p$  for fully ionized plasma with the cosmic He abundance and abundance of heavier elements set at solar. Arnaud et al. (2010) assume a heavy-element abundance that is 0.3 solar, which differs from the above value by less than 1%, a difference that is completely negligible for our purposes.

From equation 1, it is apparent that the combination  $D_A^2 Y_{SZ}$  will scale with  $C Y_X$  where  $Y_X = M_{gas} \times T_X$  (see section 3.3 for our precise definition of  $M_{gas}$  and  $T_X$ ). Thus, we expect that the  $Y_{SZ}/Y_X$  ratio is a dimensionless number that is close to unity. Throughout this work, we will often speak about the  $Y_{SZ}/Y_X$  ratio in this fashion. In practice, however,  $Y_{SZ}$  and  $Y_X$  are cluster observables that are related via a probability distribution  $P(Y_{SZ}|Y_X)$ . Here, we assume  $P(Y_{SZ}|Y_X)$  is a log-normal distribution, which takes the form

$$\langle \ln(D_A^2 Y_{SZ}) | Y_X \rangle = a + \alpha \ln C Y_X. \quad (3)$$

When we speak of “the  $Y_{SZ}/Y_X$  ratio”, we mean the quantity  $\langle \ln(D_A^2 Y_{SZ}) | Y_X \rangle - \ln C Y_X$  evaluated at the pivot point of the sample. Note that if we select units such that  $C Y_X = 1$  at the pivot point, then the  $Y_{SZ}/Y_X$  ratio is just the amplitude  $a$ . We will work primarily in units of  $C Y_X = 8 \times 10^{-5} \text{ Mpc}^2$ , corresponding to the pivot point for the *Chandra-Planck* cluster sample (see section 3). For brevity, we will often simply write  $\ln(Y_{SZ}/Y_X)$  — as opposed to the full  $\langle \ln D_A^2 Y_{SZ} | Y_X \rangle - \ln C Y_X$  expression — to denote the  $Y_{SZ}/Y_X$  ratio.

## 2. X-RAY PREDICTIONS

Equation 1 allows one to compute the  $Y_{SZ}$  signal of a galaxy cluster based on the gas and temperature profiles of galaxy clusters. With sufficiently high quality X-ray data, both of these profiles can be observationally constrained, allowing one to directly predict the  $Y_{SZ}$  signal of a galaxy cluster from the X-ray data. Using this method, Arnaud et al. (2010) predicted that  $D_A^2 Y_{SZ}/C Y_X = 0.924$  or  $\ln(Y_{SZ}/Y_X) = -0.08$  when  $T_X$  is defined within a  $[0.15, 0.75] R_{500}$  aperture. Using the Vikhlinin et al. (2006) *Chandra* results for local relaxed clusters, we predict nearly the same ratio. Specifically, the mass-weighted temperature

$$T_{mw} = \frac{\int dV \rho_{gas}(\mathbf{x}) T(\mathbf{x})}{\int dV \rho_{gas}(\mathbf{x})}, \quad (4)$$

is related to the spectroscopic temperature  $T_X$  via  $T_{mw}/T_X = 0.928$ , where  $T_X$  is measured in the  $[0.15 - 1] R_{500}$  aperture. Using the definition for  $T_{mw}$ , we see that we can rewrite equation 1 via

$$D_A^2 Y_{SZ} = C M_{gas} T_{mw}, \quad (5)$$

from which we find  $\ln(Y_{SZ}/Y_X) = -0.07$ .

It is potentially a concern that the Arnaud et al. (2010) work is based on a representative cluster sample of X-ray

luminous clusters while Vikhlinin et al. (2006) include only relaxed, cool core clusters. However, empirically, there is very little difference in  $Y_{SZ}/Y_X$  for relaxed and unrelaxed clusters judging either from the X-ray predictions (Fig.9 in Arnaud et al. 2010) or the actual measurements (see Fig.4 in Planck Collaboration 2011a, and our results below). Another point of concern is slightly different apertures for  $T_X$  used in the *XMM* and *Chandra* samples. One expects that mean (emission-weighted) temperatures in the  $[0.15 - 1] R_{500}$  and  $[0.15 - 0.75] R_{500}$  annuli should be close because only a small fraction of the total X-ray flux comes from outside  $0.75 R_{500}$ . Indeed, the  $T_X([0.15, 0.75]R_{500})/T_X([0.15, 1]R_{500})$  ratios in the *Chandra* sample of Vikhlinin et al. (2009) are within  $\pm 0.015$  of a mean value of 0.985. An analysis of the deeper pointings among the ESZ-*XMM* sample (G.Pratt, private comm.) shows a similar value, even though the temperature ratio for the REXCESS sample (Pratt et al. 2009) was somewhat lower on average ( $\approx 0.95$ ), and showed a larger spread  $0.85 - 1$ . We proceed accordingly, and ignore the difference in the definition of TX between the two works. With this caveat in mind, we conclude that both *XMM* and *Chandra* predict  $\ln(Y_{SZ}/Y_X) \simeq -0.075$  because of non-isothermal cluster temperature profiles.

There is, however, an additional complication that modifies these expectations. Specifically, when one estimates  $M_{gas}$  from X-ray data, one uses the fact that the surface brightness  $S \propto \rho_{gas}^2$  to estimate  $\langle \rho_{gas}^2 \rangle$ , averaged in radial annuli. For a uniform, spherically symmetric distribution  $\langle \rho_{gas}^2 \rangle = \langle \rho_{gas} \rangle^2$ , so one can recover the gas density profile. In practice, however, one will typically have  $\langle \rho_{gas}^2 \rangle > \langle \rho_{gas} \rangle^2$ . The clumping factor  $Q^2$  is defined via

$$Q^2 = \frac{\langle \rho_{gas}^2 \rangle}{\langle \rho_{gas} \rangle^2}, \tag{6}$$

so that  $M_{gas}^{obs} = Q M_{gas}^{true}$ . By definition,  $Y_X = M_{gas}^{obs} T_X$ , so the  $Y_{SZ}$  to  $Y_X$  ratio takes the form

$$\frac{D_A^2 Y_{SZ}}{C Y_X} = \frac{1}{Q} \frac{T_{mw}}{T_X}. \tag{7}$$

In practice, the clumping factor  $Q$  depends on radius, and the factor  $1/Q$  characterizes the mean clumping correction over the radius  $R_{500}$ . Based on this discussion, we modify our X-ray expectation by a factor of  $Q^{-1}$ . If there is no substructure masking in the X-ray analysis,  $Q$  can be very large (e.g.  $Q = 1.16$ , Mathiesen et al. 1999), though analysis of numerical simulations that include substructure masking achieve significantly lower values of  $Q$ . Based on the analysis of Nagai et al. (2007), we set  $Q = 1.05 \pm 0.05$ , where the error is set to the size of the correction to account for systematic uncertainties in the simulation physics. The corresponding expectation for the  $Y_{SZ}/Y_X$  ratio is  $\ln(D_A^2 Y_{SZ}/C Y_X) = -0.125 \pm 0.05$ .

Finally, we note that  $T_X$  measured in the X-ray can be subject to a systematic uncertainty, related to, e.g., absolute calibration of the X-ray telescope effective area. Assuming for simplicity that this results in a uniform bias of observed temperatures,  $T_X^{(meas)} = A T_X^{(true)}$ , the

measured ratio of the  $Y$ 's can be factorized as

$$\frac{D_A^2 Y_{SZ}}{C Y_X} = \frac{1}{A Q} \frac{T_{mw}}{T_X}. \tag{8}$$

Discussion of the calibration-related uncertainties in  $T_X$  is beyond the scope of this paper and we proceed assuming  $A = 1$ . However, it is important to keep in mind a possibility of a few percent systematic error in the X-ray temperature measurements with the current calibration of the *XMM-Newton* and *Chandra* instruments. To give a handle of possible deviations of  $A$  from unity, we note that within the sample we consider in this work, the average ratio of *XMM* and *Chandra*-measured temperatures for the same cluster is  $\ln(T_{XMM}/T_{Chandra}) = -0.08$  (for a detailed comparison of *XMM* and *Chandra* data on a cluster-by-cluster basis see Rozo et al. 2012, in preparation).<sup>5</sup>

### 3. DATA

#### 3.1. Cluster Sample

The cluster sample employed in this work is a subset of the Early SZ (ESZ) sample published in Planck Collaboration (2011d). The ESZ sample is comprised of 189 cluster candidates identified in a blind, multi-frequency search of the all-sky maps obtained from the first ten months of observations of the *Planck* mission (Planck Collaboration 2011e). The threshold for cluster detection was set at a signal-to-noise ( $S/N$ )  $\geq 6$ . This ESZ sample was searched for archival *XMM* data, and a sub-sample of 88 galaxy clusters with *XMM* data were identified. Of these, 62 clusters were processed in time for publication, as detailed in Planck Collaboration (2011a). Starting from this sub-sample of 62 galaxy clusters, we identified 28 clusters with *Chandra* data that had already been analyzed using the data reduction pipeline of Vikhlinin et al. (2009). The analysis presented here is based on this sub-sample of 28 galaxy clusters, which is summarized in Table 1. 20 of these are relaxed galaxy clusters, and 8 are merging systems. A plot of the  $Y_{SZ}$  vs  $Y_X$  data for the galaxy clusters is shown in Figure 1.

#### 3.2. Planck Data

For each of our galaxy clusters, (Planck Collaboration 2011a) estimated the integrated Compton parameter  $Y_{SZ}$  using a matched-filter algorithm. The matched filter assumes an Arnaud et al. (2010) pressure profile, which is used to predict the CMB temperature perturbation  $\delta T(\theta)$  of each galaxy cluster in each of the *Planck* frequency bands. In order to perform the fit, the clusters are first assigned a putative  $R_{500}$  radius based on the *XMM* X-ray data and the  $M-Y_X$  scaling relation of Arnaud et al. (2010). The amplitude of the matched-filter, which can be expressed in terms of the integrated Compton parameter  $Y_{SZ}$ , is then fit using the temperature data within a projected aperture of  $5R_{500}$ . We note that the shape of the matched filter is held fixed in the Planck Collaboration (2011a) analysis, but their systematic tests demonstrate that varying the shape of the filter within tolerable levels does not significantly impact

<sup>5</sup> The quoted ratio does *not* correct for the difference between the temperature definitions used in the relevant *XMM* and *Chandra* works as noted earlier.

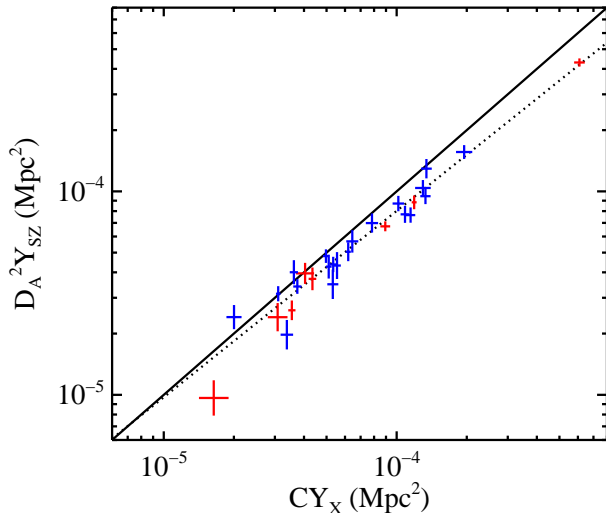


FIG. 1.— The relation between the Planck  $D_A^2 Y_{SZ}$  and *Chandra*  $CY_X$  measured in the same aperture,  $R_{500}$  provided by *XMM-Newton* mass estimates. Blue and red crosses represent dynamical relaxed and merging clusters, respectively (per the Vikhlinin et al. (2009) classification). The solid line shows a 1-1 relation, while the dotted line is our best fit relation. The amplitude at the pivot point corresponds to  $D_A^2 Y_{SZ}/CY_X = 0.82$ .

the recovered scaling relations. The median error in the recovered  $Y_{SZ}$  values for our cluster sample is 11%, and systematic uncertainties due to instrumental beam size and radio point source contamination are all expected to be at the few percent level at most. Note that because Planck Collaboration (2011a) assumed  $h = 0.7$  while we assume  $h = 0.72$ , we must rescale the  $D_A^2 Y_{SZ}$  values in Planck Collaboration (2011a) appropriately. Further, the Planck team uses the redshifts listed for the clusters in the NED and SIMBAD databases while we use the redshifts of the dominant central galaxies. We believe the latter approach is more robust because it allows one to avoid contamination by projection effects in some cases. Therefore, we rescaled all angular diameter distances to our adopted  $z$  values. The cluster redshifts, along with the rescaled  $Y_{SZ}$  values, are detailed in Table 1.

### 3.3. *Chandra* Data

Our analysis is based on the sub-sample of ESZ galaxy clusters from Planck Collaboration (2011d) that have *Chandra* data that was reduced as part of the work in Vikhlinin et al. (2009), described in full detail in Vikhlinin et al. (2005, 2006). Here, we provide only a brief summary. We note that not all galaxy clusters in our analysis are included in the Vikhlinin et al. (2009) sample. These are the clusters which were analyzed by Vikhlinin et al. (2009) but not included in the flux-limited sample used in their cosmological analysis. The full list of clusters employed in our analysis is presented in Table 1.

We use the available *Chandra* data to estimate  $Y_X = M_{gas} \times T_X$  for each of the clusters in our sample, where  $M_{gas}$  is the total gas mass within the radius  $R_{500}$  employed by Planck Collaboration (2011a), and  $T_X$  is the spectroscopic temperature within an annulus  $R \in [0.15, 1]R_{500}$ . To estimate  $M_{gas}$ , we rely on ana-

lytic fits to the gas density profiles of individual clusters. The fits were based on the X-ray brightness profiles in the 0.7–2 keV energy band measured with *Chandra* and *ROSAT* PSPC (see Vikhlinin et al. (2009) for details). All detectable X-ray substructures were masked out from the profile measurements to minimize the impact of gas clumping. The X-ray flux in the 0.7–2 keV band is very insensitive to the plasma temperature so long as  $T \gtrsim 2$  keV, as in the case of the sample under consideration. Nevertheless, we apply the appropriate temperature and metallicity corrections to the X-ray profile to estimate  $M_{gas}$ . The mean cluster temperature reported by Vikhlinin et al. (2009) corresponds to the single-temperature fit to the X-ray spectrum in the 0.6–10 keV band extracted within an annulus  $[0.15, 1]R_{500}$ . The median error in the recovered  $Y_X$  values for our cluster sample is 3%, nearly identical to the median error in the corresponding *XMM* X-ray data in Planck Collaboration (2011a).

### 3.4. On the Importance of Apertures

As already mentioned in section 1.1, we ignore any radial dependence on the  $Y_{SZ}-Y_X$  scaling relation. In other words, we are explicitly assuming that the parameters  $a$  and  $\alpha$  are insensitive to the radius at which both  $Y_{SZ}$  and  $Y_X$  are evaluated. This is clearly not true over arbitrarily large radial ranges, but we expect any evolution over the range of radii probed to be at the  $\lesssim 1\%$  level, so long as both  $Y_{SZ}$  and  $Y_X$  are always measured within the same aperture. Since we rely on the SZ data from Planck Collaboration (2011a), we have to use the same metric apertures adopted in that work. Specifically, to estimate  $Y_X$ , we first measure  $M_{gas}$  within the assigned  $R_{500}$  aperture, and multiply this by the estimated temperature  $T_X$  as quoted in Vikhlinin et al. (2009). We do not remeasure  $T_X$  since the X-ray temperature is robust to modest changes in the assigned  $R_{500}$  radius of a cluster. A relation between *Planck*-measured  $Y_{SZ}$  and the *Chandra*  $Y_X$  values is shown in Fig. 1. There is an obvious, tight correlation that is nearly linear, with no obvious offset between merging and relaxed systems.

## 4. LIKELIHOOD MODEL

Because we will be assuming log-normal models throughout, we begin by defining  $y_x$  and  $y_{sz}$  via

$$y_x = \ln \left( \frac{CY_X}{8 \times 10^{-5} \text{ Mpc}^2} \right) \quad (9)$$

$$y_{sz} = \ln \left( \frac{D_A^2 Y_{SZ}}{8 \times 10^{-5} \text{ Mpc}^2} \right). \quad (10)$$

We divide both  $Y_X$  and  $Y_{SZ}$  by  $8 \times 10^{-5} \text{ Mpc}^2$  so that both quantities are still measured in the same units, while simultaneously shifting the pivot point of the  $y_{sz}-y_x$  scaling relation to ensure the amplitude and slope of the best-fit  $Y_{SZ}-Y_X$  relation are nearly uncorrelated.

For each cluster, we assume that the observed  $y_x$  value is given by

$$y_x = \bar{y}_x + \delta_y \quad (11)$$

where  $\bar{y}_x$  is the true value, and  $\delta_y$  is a random gaussian fluctuation of zero mean and  $\langle \delta_y^2 \rangle = \sigma_x^2$ , where  $\sigma_x$  is the assigned observational error. A similar expression holds

for  $y_{sz}$  in terms of the true  $SZ$  signal  $\bar{y}_{sz}$ . The true values  $\bar{y}_{sz}$  and  $\bar{y}_x$  are themselves related via a probability distribution  $P(\bar{y}_{sz}|\bar{y}_x)$  that characterizes the scaling relation. We assume this is a log-normal distribution of mean

$$\langle y_{sz}|y_x \rangle = a + \alpha y_x \quad (12)$$

and variance  $\sigma_{sz|x}^2$ , so that  $\sigma_{sz|x}$  is the intrinsic scatter in the  $Y_{SZ}-Y_X$  relation. We assume this scaling relation is redshift independent, so  $a$ ,  $\alpha$ , and  $\sigma_{sz|x}$  are all redshift independent. Note that because we have chosen our units to ensure that  $y_x = 0$  at  $CY_X = 8 \times 10^{-5}$  Mpc<sup>2</sup>, the amplitude  $a$  is the  $Y_{SZ}/Y_X$  ratio at this scale.

The probability that a galaxy cluster has observed values  $y_x$  and  $y_{sz}$  can be written as

$$P(y_{sz}, y_x) = \int d\bar{y}_x d\bar{y}_{sz} P(y_{sz}, y_x | \bar{y}_{sz}, \bar{y}_x) P(\bar{y}_{sz}, \bar{y}_x) \quad (13)$$

$$= \int d\bar{y}_x d\bar{y}_{sz} P(y_{sz} | \bar{y}_{sz}) P(y_x | \bar{y}_x) P(\bar{y}_{sz} | \bar{y}_x) P(\bar{y}_x), \quad (14)$$

where we are using the fact that the observational errors in  $y_x$  and  $y_{sz}$  are uncorrelated. In principle, there can be a small amount of covariance induced by aperture effects. We discuss this effect in more detail below, but the main conclusion is that the effect is negligible for our purposes, and so we will ignore this effect in our discussion.

Note the probability  $P(y_{sz}, y_x)$  depends on the distribution  $P(\bar{y}_x)$  of the cluster sample under consideration, which depends on cluster selection effects. We consider two possibilities, namely a flat prior for the value  $\bar{y}_x$ , and a power-law distribution in  $Y_X$ , corresponding to  $P(\bar{y}_x) = \exp(-\beta y_x)$ . The slope  $\beta$  can then be set to the expected slope for a WMAP7 cosmology. In practice, neither is exact, but it can help give us a sense of the level of systematic uncertainty in our data due to selection effects.

Setting  $P(\bar{y}_x)$  to a constant, integration of equation 14 allows us to conclude that  $P(y_{sz}, y_x)$  is a Gaussian distribution

$$P(y_{sz}, y_x) = G(\delta; \sigma_{tot}^2) \quad (15)$$

$$= \frac{1}{\sqrt{2\pi\sigma_{tot}^2}} \exp\left(-\frac{1}{2} \frac{\delta^2}{\sigma_{tot}^2}\right) \quad (16)$$

where

$$\delta = y_{sz} - (a + \alpha y_x) \quad (17)$$

$$\sigma_{tot}^2 = \alpha^2 \sigma_x^2 + \sigma_{sz}^2 + \sigma_{sz|x}^2. \quad (18)$$

For a power-law distribution  $P(y_x) \propto \exp(-\beta y_x)$ , we find

$$P(y_{sz}, y_x) \propto G(\delta; \sigma_{tot}^2) \times \exp\left[-\beta(y_x f_{sz} + \tilde{y}_x f_x) + \frac{1}{2} \frac{\beta^2}{\alpha^2} \sigma_{tot}^2 f_x f_{sz}\right] \quad (19)$$

where  $\tilde{y}_x$  is the  $y_x$  value expected from  $y_{sz}$  from naively inverting the scaling relation, i.e.

$$\tilde{y}_x = \alpha^{-1}(y_{sz} - a). \quad (20)$$

$f_x$  and  $f_{sz}$  are the fraction of the total variance due to

$y_x$  and  $y_{sz}$  respectively,

$$f_x = \frac{\alpha^2 \sigma_x^2}{\sigma_{tot}^2} \quad (21)$$

$$f_{sz} = \frac{\sigma_{sz}^2 + \sigma_{sz|x}^2}{\sigma_{tot}^2}. \quad (22)$$

Note that for  $\beta = 0$  (i.e. a flat prior), we recover equation 16, as we should. For our fiducial analysis, we will assume  $\beta = 1.8$ , as appropriate for a logarithmic slope of the cumulative halo mass function  $N(M) \propto M^\gamma$  for  $\gamma = 3$ , and a self-similar slope  $M \propto Y_X^{3/5}$ . We have verified that setting  $\beta = 0.0$  does not impact our result at any significant level, which suggests our results are not sensitive to the details of the cluster selection function. This is in good agreement with the more detailed treatment of selection effects of Planck Collaboration (2011a), who find that selection effects only impacts the slope of the best-fit relation, and then only at the  $\Delta\alpha = 0.01$  level, a systematic that is three times smaller than the statistical uncertainty.

We assume that all galaxy clusters represent independent realizations of the probability distribution  $P(y_{sz}, y_x)$ , so that the likelihood of the entire data set is simply the product of the individual likelihoods. The posterior is

$$\mathcal{L}(a, \alpha, \sigma_{sz|x} | y_{sz}, y_x) \propto P_0(a, \alpha, \sigma_{sz|x}) \prod_{clusters} P(y_{sz} | y_x) \quad (23)$$

where  $P_0$  is the prior, and the product is over all clusters. Note that while we are using  $\sigma_{sz|x}$  as a model parameter in order to facilitate physical interpretation of our results, it is the variance  $\sigma_{sz|x}^2$  that is more physical, so we adopt a flat prior on  $\sigma_{sz|x}^2$ , corresponding to

$$P_0(a, \alpha, \sigma_{sz|x}) \propto \sigma_{sz|x}. \quad (24)$$

#### 4.1. Aperture Correlations

As detailed above, we have assumed that both  $Y_X$  and  $Y_{SZ}$  are estimated within the same aperture, and we have explicitly assumed that the  $Y_{SZ}/Y_X$  ratio is radius independent. This guarantees that the mean relation is always adequately sampled. However, any noise in the estimated aperture  $R_{500}$  necessarily induces correlated noise in the estimated  $Y_{SZ}$  and  $Y_X$  values for each clusters, and this covariance should in principle be included in the analysis. In practice, however, this is difficult to achieve because the  $Y_X$  aperture adopted is that of Planck Collaboration (2011a) rather than the  $R_{500}$  aperture that we would assign based on the  $Y_X$  measurements of Vikhlinin et al. (2009). This makes developing a self-consistent model that accounts for this covariance difficult. We can demonstrate, however, that we expect this effect to be negligible.

To see this, we go back to equation 11. We now let  $\bar{y}_x$  be the true  $y_x$  value at the true radius  $R_{500}$ , while  $\bar{y}_x(R)$  is the true  $y_x$  value at radius  $R$ . Assuming a power-law scaling

$$\bar{y}_x(R) = \bar{y}_x + \gamma_x \ln\left(\frac{R}{R_{500}}\right), \quad (25)$$

and letting the observed  $R_{500}$  radius be a power-law as

a function of the observed  $Y_X$ , one has

$$\ln\left(\frac{R_{obs}}{R_{500}}\right) = \tau(y_x - \bar{y}_x) \quad (26)$$

where  $\tau$  is some proportionality constant. Our modified equation 11 is

$$y_x = \bar{y}_x(R) + \delta_x, \quad (27)$$

so putting it all together, we arrive at

$$y_x = \bar{y}_x + \frac{1}{1 - \gamma_x \tau} \delta_x. \quad (28)$$

The gas density profile of galaxy clusters is such that  $\gamma_x = 1.2$ , and for a self-similar scaling,  $R \propto M^{1/3} \propto Y_X^{1/5}$ , so  $\tau = 0.2$ . Thus, if we self-consistently estimated the radius  $R_{500}$  from  $Y_X$ , we would find that the variance in  $Y_X$  increases by  $\approx 25\%$ . Since the variance in  $Y_{SZ}$  is much larger than that in  $Y_X$ , this is not a source of concern.

What about the impact these fluctuations have on  $Y_{SZ}$ ? A similar argument as the one above results in

$$y_{sz} = \bar{y}_{sz} + \frac{\gamma_{sz}\tau}{1 - \gamma_{sz}\tau} \delta_x + \delta_{sz}. \quad (29)$$

Thus, the fluctuations in  $y_{sz}$  are now explicitly correlated with those in  $y_x$ . Note, however, that  $\delta_x \ll \delta_{sz}$  because the SZ measurements are noisier, and that the  $\delta_x$  fluctuations are themselves down-weighted by a factor  $\approx 0.3$ . This is a very minor perturbation to the variance in  $y_{sz}$ , and the correlation coefficient between  $y_x$  and  $y_{sz}$  induced in this manner is very small indeed. To first order in  $\gamma_{sz}\tau$  and  $\gamma_x\tau$  we find

$$r \approx \gamma_{sz}\tau \frac{\sigma_x}{\sigma_{sz}} \approx 0.06. \quad (30)$$

Thus, we expect the covariance induced from a self-consistent estimate of  $R_{500}$  to be negligible in this case. This independence is further strengthened by the fact that  $R_{500}$  is not estimated from the *Chandra* data itself, so while we cannot adequately model the effects of aperture choice on the variance of our measurements, we do not expect these to impact our results at any significant level.

## 5. RESULTS

We evaluate the posterior on a grid in the 3-dimensional space spanned by the parameters  $a$ ,  $\alpha$ , and  $\sigma_{sz|x}$ , where the range of parameters is chosen to as to ensure that it does not impact our results. We use  $a \in [-0.35, -0.05]$ ,  $\alpha \in [0.8, 1.1]$ , and  $\sigma_{sz|x} \in [0, 0.25]$ .<sup>6</sup>

Figure 3 shows our best fit scaling relation. The best fit amplitude (i.e. the  $Y_{SZ}/Y_X$  ratio), slope, and scatter are

$$a = -0.202 \pm 0.028 \quad (31)$$

$$\alpha = 0.916 \pm 0.035 \quad (32)$$

$$\sigma_{sz|x} = 0.082 \pm 0.035. \quad (33)$$

<sup>6</sup> In section 6, we repeat our analysis using data published in Planck Collaboration (2011a). When doing so, we always make sure the extent of our multidimensional grid completely covers the high-likelihood regions in parameters space.

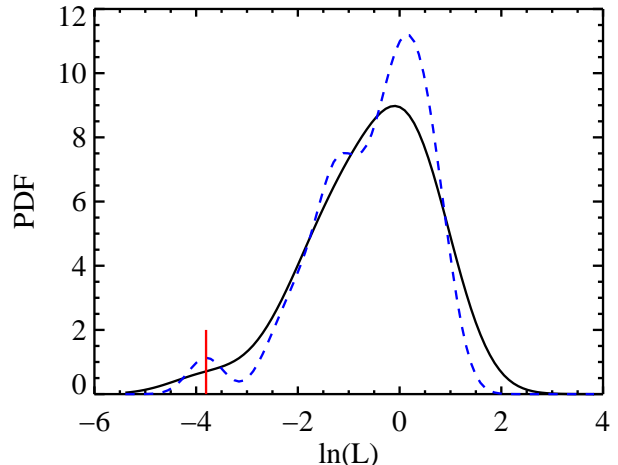


FIG. 2.— The distribution of the log-likelihood value from our cluster sample. We use our best fit model to evaluate the log-likelihood of each clusters, and a Gaussian Kernel Density Estimator (KDE) to estimate the density distribution. The black line uses Silverman’s rule of thumb to set the width of the KDE (i.e. the width of the Gaussian is set to  $1.34\sigma/N^{0.2}$  where  $N$  is the number of samples). The dashed blue curve halves this width, and is obviously under-smoothed. There are no glaring outliers. The most discrepant cluster is A2163 (solid red line), which has a low likelihood because of it’s extremely large mass.

In all cases, the quoted values are the mean of the distribution, and the error is the standard deviation of the marginalized distribution. The slope is marginally consistent with  $\alpha = 1$  ( $\approx 2.3\sigma$  offset).

We have tested the sensitivity of our result to outliers by performing jackknife resamples of our galaxy clusters, and repeating our analysis. The resulting mean and standard deviation are

$$a = -0.202 \pm 0.024 \quad (34)$$

$$\alpha = 0.916 \pm 0.032 \quad (35)$$

$$\sigma_{sz|x} = 0.083 \pm 0.021 \quad (36)$$

The central values and error estimates are essentially identical to those derived from our full likelihood analysis, demonstrating that there are no large outliers. This can be furthered evidence by evaluating the log-likelihood of each individual cluster. The distribution of log-likelihoods is shown in Figure 2. The least likely cluster is A2163, reflecting the extremely large mass of this system. By the same token, A2163 significantly increases the lever-arm with which the slope of the  $Y_{SZ}-Y_X$  relation can be constrained, and has an important impact on the fit. Removing A2163 from the fit results in a slope  $\alpha = 0.906 \pm 0.046$ . The error increases significantly, but the deviation of  $\alpha$  from unity is still  $2\sigma$ .

We test whether the scatter of the  $Y_{SZ}-Y_X$  relation is consistent with zero or not by focusing not on the scatter, but on the variance,  $\sigma_{sz|x}^2$ , which is the more physical parameter. The marginalized likelihood for the variance  $\sigma_{sz|x}^2$  is shown in Figure 4. We see that the data is consistent with zero variance. We can place an upper limit on the variance,  $\sigma_{sz|x}^2 \leq 0.021$  (95% CL), corresponding to  $\sigma_{sz|x} \leq 0.144$ .

We also explicitly consider the  $Y_{SZ}-Y_X$  relation with

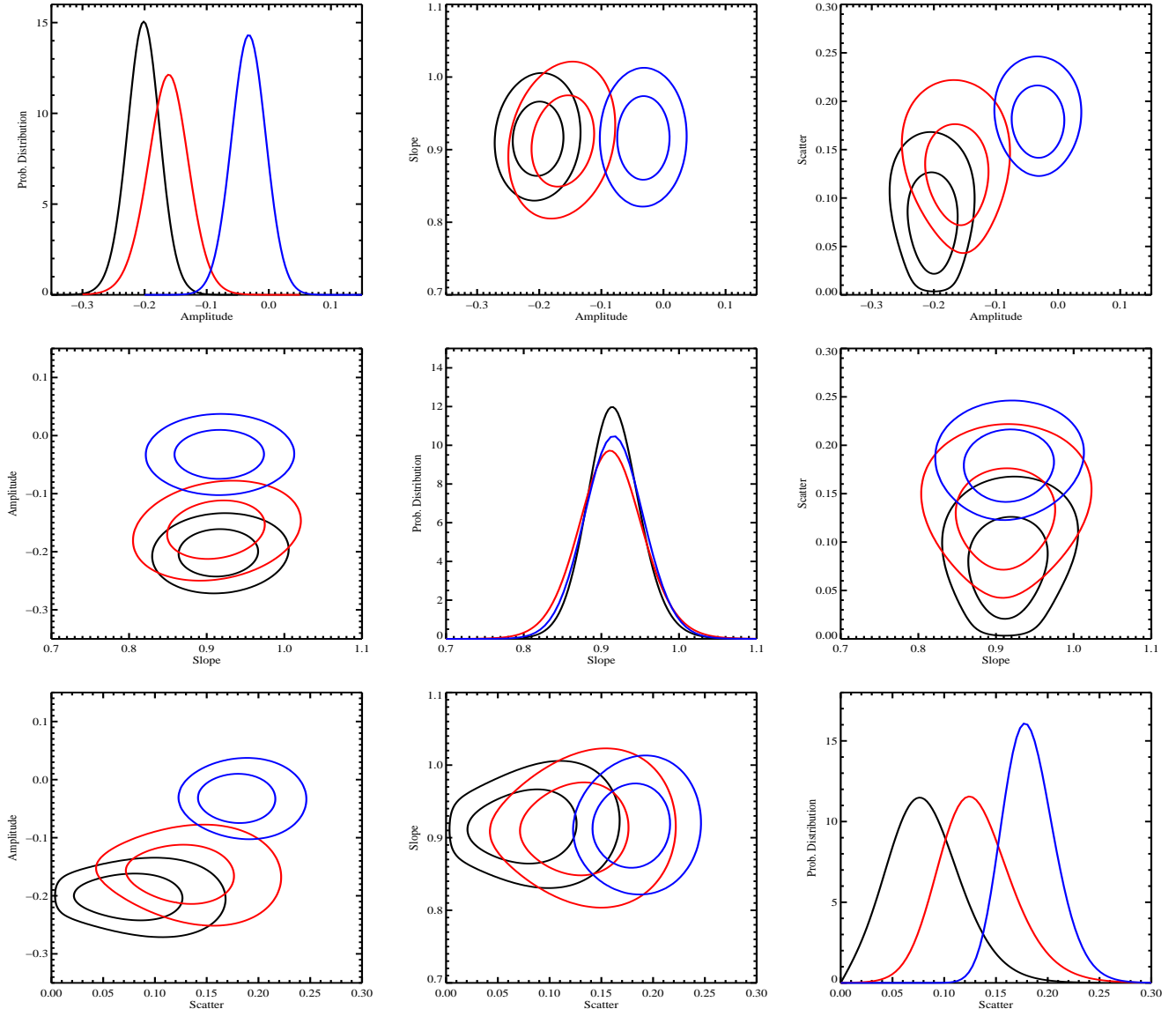


FIG. 3.— Best-fit parameters for the  $Y_{SZ}-Y_X$  scaling relation. Black curves are obtained using *Chandra* data and the cluster sample in Table 1. Red and blue curves are using the *Planck* Collaboration (2011a) data. The red curves show the results when we restrict our analysis of the *Planck* Collaboration (2011a) data to the same galaxy clusters that constitute our *Chandra* sample. The blue curves include all galaxy clusters in *Planck* Collaboration (2011a). All confidence regions are 68% and 95% likelihood contours respectively.

a fixed slope of unity ( $\alpha = 1$ ). The scatter is somewhat increased to  $\sigma_{sz|x} = 0.120 \pm 0.033$ . The uncertainty in the amplitude also increases, reflecting the additional intrinsic scatter required to fit all the data. We find  $a = -0.201 \pm 0.032$ . In this context, we also investigate whether the resulting amplitude is sensitive to the dynamical state of the galaxy clusters. We split the clusters depending on whether they are relaxed or unrelaxed, using the same criteria employed in Vikhlinin et al. (2009). The best fit amplitude for the relaxed and unrelaxed cases is  $a = -0.17 \pm 0.04$  and  $a = -0.26 \pm 0.06$ , consistent with no systematic offset between the two.

## 6. DISCUSSION

### 6.1. Comparison to Previous Work

We compare our best fit  $Y_{SZ}-Y_X$  scaling relation to other empirical investigations of the  $Y_{SZ}/Y_X$  ratio.

There are several analysis of the SZ and X-ray properties of galaxy clusters, but most cannot be straight forwardly compare to ours. Bonamente et al. (2008) do not explicitly consider the  $Y_{SZ}-Y_X$  relation, but simply note that an isothermal model with no gas clumping gives a good fit to their data. This model corresponds to  $\ln(Y_{SZ}/Y_X) = 0$ , which is in strong conflict with our results. We note, however, that they used significantly smaller apertures ( $R_{2500}$ ), and that their SZ and X-ray estimators are explicitly linked in the analysis: the SZ data helps constrain the X-ray data model and vice-versa, and the isothermal  $\beta$  model effectively acts as a prior relating the two data sets. Thus, it is difficult to fairly compare their analysis to ours.

On a similar vein, Comis et al. (2011) used the ACCEPT cluster catalog (Cavagnolo et al. 2009) to probe the  $Y_{SZ}-Y_X$  relation, but within an overdensity  $\Delta =$

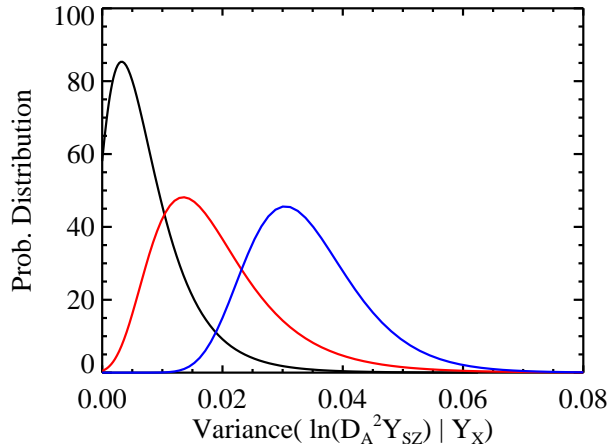


FIG. 4.— Likelihood distribution for the intrinsic variance in  $\ln Y_{SZ}$  at fixed  $Y_X$ . Black, red, and blue curves are for the *Chandra*–*Planck* data, the *XMM*–*Planck* data restricted to the subset of clusters with *Chandra* data, and the full *XMM*–*Planck* data set.

2500. In addition, Comis et al. (2011) do not exclude the core when estimating  $T_X$ , which is expected to introduce scatter, and to systematically bias the  $Y_X$  measurements relative to what would be measured using core-excluded temperatures. Indeed, Comis et al. (2011) find both higher scatter and a higher  $Y_{SZ}/Y_X$  ratio, as we would expect. A more quantitative comparison with our results, however, is difficult.

The Planck Collaboration (2011a) analysis is the one that is closest in spirit to ours. Further, our analysis relies on their SZ-data. Switching the best fit amplitude reported in that work to the pivot point adopted here, their best fit scaling relation corresponds to  $a = -0.037 \pm 0.023$  and  $\alpha = 0.96 \pm 0.04$ . This amplitude is significantly higher than ours at more than  $4.5\sigma$ . Their slope is steeper, but consistent with ours. There is also tension between the recovered scatter of their analysis and ours, with the  $\sigma_{sz|x} = 0.228$  value reported by Planck Collaboration (2011a) being ruled out by our data at very high significance.<sup>7</sup>

What drives the difference between our results and those of Planck Collaboration (2011a)? Two obvious possibilities that we can readily explore are the fitting method used to recover the scaling relation, and the fact that we use a subsample (28 out of 62) of the galaxy clusters employed in the Planck Collaboration (2011a) analysis.

We test the importance of the fitting method by re-fitting the Planck Collaboration (2011a) data with our likelihood method. We find  $a = -0.032 \pm 0.028$ ,  $\alpha = 0.917 \pm 0.039$ , and  $\sigma_{sz|x} = 0.182 \pm 0.025$ . For this analysis, we have used the data exactly as reported in Planck Collaboration (2011a), that is, we use their redshifts, and we assume  $h = 0.70$ , though we note that the  $h$  value impact the amplitude  $a$  only at the 1% level. The only exception is cluster A2034, for which the redshift in Planck Collaboration (2011a) is clearly incorrect (Planck Collaboration 2011a, quote  $z = 0.151$ ,

<sup>7</sup> The number quoted in Planck Collaboration (2011a) is  $0.10 \pm 0.010$ , but they quote scatter in dex, while we quote the scatter in  $\ln Y_{SZ}$ .

while we use the cD galaxy redshift,  $z = 0.113$ , a very significant difference). These results are illustrated with the blue lines in Figure 3. Our best fit amplitude is in agreement with that quoted in Planck Collaboration (2011a), though our best fit value for the intrinsic scatter is lower, with  $\Delta\sigma_{sz|x} \approx 0.04$  (partly because we have corrected the redshift of cluster A2034), and our best fit slopes are flatter. Despite the differences noted above, we can conclude that the fitting method is not responsible for the difference between our results and those of Planck Collaboration (2011a).

We test the importance of using a subsample of Planck Collaboration (2011a) data by analyzing the Planck Collaboration (2011a) data, but restricting our analysis to the clusters employed in our *Chandra* analysis. In this case, we find  $a = -0.166 \pm 0.035$ ,  $\alpha = 0.912 \pm 0.043$ , and  $\sigma_{sz|x} = 0.132 \pm 0.036$ . We see that the sample selection plays a significant impact on the results of the recovered  $Y_{SZ}/Y_X$  ratio for the *XMM* data. The higher normalization of the  $Y_X - Y_{SZ}$  relation from the full *Planck* sample must therefore be driven by the remaining 34 clusters not in the *Chandra* subsample (most of which are at  $z > 0.1$ ). Note that while we have not attempted to replicate the Monte Carlo analysis of Planck Collaboration (2011a) to try to estimate selection effects, their own tests suggest that there are negligible, having no impact on the amplitude of the  $Y_{SZ}-Y_X$  relation, and impacting the slope only at the  $\Delta\alpha = 0.01$  level, much less than the statistical uncertainty in the measurement.

Even when restricting ourselves to the same galaxy clusters, however, the *Chandra* data results in a lower  $Y_{SZ}/Y_X$  ratio. While this difference is  $< 1\sigma$  in terms of the statistical error bar, we note the statistical significance is significantly higher because both data sets share the same  $Y_{SZ}$  data, and it is the  $Y_{SZ}$  error that dominates the error budget. More specifically, the fact that both clusters use the exact same  $Y_{SZ}$  data implies that the the difference must be driven entirely by systematic differences in  $Y_X$  between the two data sets.

Aside from the differences in amplitude, it is interesting to note the difference in the intrinsic scatter estimate between the two data sets. The simplest interpretation of this result is that there are unidentified sources of stochasticity in the Planck Collaboration (2011a) X-ray analysis that result in an overestimate of the intrinsic scatter of the  $Y_{SZ}-Y_X$  relation of galaxy clusters.

Finally, it is worth noting that all of our fits consistently return a slope  $\alpha \approx 0.91$ , compared to the  $\alpha = 0.96$  slope reported in Planck Collaboration (2011a). This difference appears to be due to the choice of fitting method: fitting our data using the same BCES method employed by Planck Collaboration (2011a), we recover  $\alpha = 0.96$ . Since we find no evidence for non-gaussian scatter intrinsic scatter in the  $Y_{SZ} - Y_X$  relation, and furthermore, the observed scatter is dominated by measurement uncertainties, we believe that using the maximum likelihood fit is better justified.

The final data set that we compare against is that of Andersson et al. (2010), who find  $\ln Y_{SZ}/Y_X = -0.20 \pm 0.1$  using *Chandra* X-ray data and SPT SZ data with a median cluster redshift  $z \approx 0.7$ . This value is essentially in perfect agreement with ours, and is also consistent



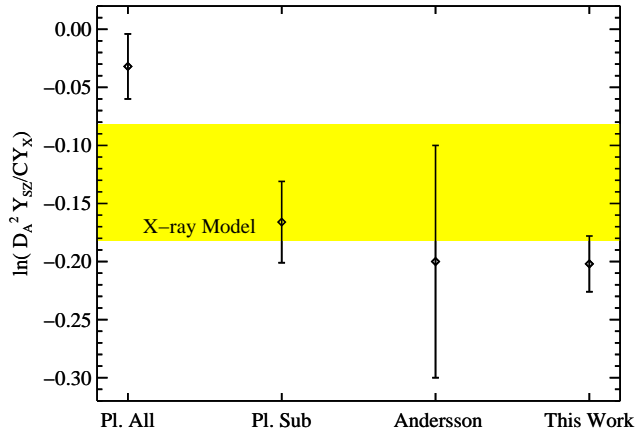


FIG. 5.— The  $Y_{SZ}/Y_X$  ratio, as observed using a variety of data. The horizontal band is our X-ray predictions model from section 2, the width of which ( $\pm 0.05$ ) reflect our ignorance of clumping corrections. The “Pl. All” data point shows our re-analysis of the Planck Collaboration (2011a) data. “Pl. Sub” uses this same data, but restricts the cluster sample to that employed in our *Chandra* analysis. The Andersson point comes from Andersson et al. (2010).

with that of Planck Collaboration (2011a). The uncertainty in their measurement is significantly larger than the one reported here or in Planck Collaboration (2011a) both because of a smaller cluster sample, and because the X-ray data is also shallower in terms of number of X-ray photons. We conclude that from the comparison of *Planck*+*Chandra* and SPT+*Chandra* samples, there is no evidence for evolution in the  $Y_{SZ} - Y_X$  relation. It will be interesting to make the same comparison in the future as both projects acquire more galaxy clusters with high quality SZ and X-ray data.

For completeness, we have also estimated the amplitude of the  $Y_{SZ}-Y_X$  relation setting  $\alpha = 1$  for both our data, and the various sub-samples of the Planck Collaboration (2011a) data we considered here. The likelihood for each of these fits is shown in Figure 6. In addition, we also computed the best fit amplitude for the low redshift ( $z \leq 0.12$ ) and intermediate redshift ( $0.12 < z < 0.3$ ) sub-samples from Planck Collaboration (2011a). Our results are summarized in Figure 5.

### 6.2. Comparison to X-ray Expectations

Our empirical calibration of the  $Y_{SZ} - Y_X$  relation for  $z < 0.1$  Planck clusters is somewhat lower than the expectation from the observed cluster temperature profiles for both *Chandra* and *XMM* measurements,  $\Delta \ln(Y_{SZ}/Y_X)_{XMM} = -0.09 \pm 0.035$  and  $\Delta \ln(Y_{SZ}/Y_X)_{Chandra} = -0.127 \pm 0.024$ . Some of this offset can be explained by small-level nonuniformities of the intracluster gas (gas clumping factor  $Q$  in eq. 8). As per our earlier discussion, we set  $Q = 1.05 \pm 0.05$  (Nagai et al. 2007), which brings the predicted  $Y_{SZ}/Y_X$  ratio within a few percent of the observed value,  $\Delta \ln(Y_{SZ}/Y_X)_{XMM} = 0.09$  for the full *XMM-Planck* cluster sample,  $\Delta \ln(Y_{SZ}/Y_X)_{XMM} = -0.042 \pm 0.035$  for the *Chandra* sub-sample of galaxy clusters, and  $\Delta \ln(Y_{SZ}/Y_X)_{Chandra} = -0.078 \pm 0.024$  as estimated from *Chandra*. Note that the estimated systematic uncertainty in the clumping correction is  $\pm 0.05$ , so all val-

ues are in reasonable agreement with expectations, even though some are in strong statistical tension with one another.

Our results fit within the general picture that has developed in the recent past. A few years back, a variety of works argued that the SZ signal of galaxy clusters was inconsistent with predictions from X-ray data (Lieu et al. 2006; Bielby & Shanks 2007). These authors fit isothermal  $\beta$  models to *ROSAT* data in order to predict the SZ-signal of galaxy clusters as observed by WMAP, finding that the observed SZ signal was significantly lower than that their predictions. There is now ample evidence that  $\beta$  models are inadequate fits to the intra-cluster gas of galaxy clusters (e.g Vikhlinin et al. 2006; Croston et al. 2008), and that clusters are not isothermal (e.g. Vikhlinin et al. 2006; Pratt et al. 2007; Sun et al. 2009; Moretti et al. 2011). Hallman et al. (2007) and Mroczkowski et al. (2009) explicitly demonstrated that isothermal model fits to X-ray data leads one to over-predict the SZ signal of galaxy clusters. Using more realistic density and temperature profiles, one finds good agreement between SZ and X-ray observables (Atrio-Barandela et al. 2008; Komatsu et al. 2008; Mroczkowski et al. 2009; Diego & Partridge 2010; Zwart et al. 2011; Melin et al. 2011; Planck Collaboration 2011a,c). The results summarize above fit well within this new wave of works.

## 7. SUMMARY AND CONCLUSIONS

Using SZ data from *Planck* (Planck Collaboration 2011a) and X-ray data from *Chandra* (Vikhlinin et al. 2009), we have estimated the  $Y_{SZ}-Y_X$  scaling relation. Assuming a power-law of the form in equation 12, we find  $\ln(Y_{SZ}/Y_X) = a = -0.202 \pm 0.024$ ,  $\alpha = 0.916 \pm 0.032$ , and  $\sigma_{sz|x} = 0.083 \pm 0.021$ . The scatter constraint is prior-driven, and the variance in the relation is consistent with zero intrinsic scatter. The slope  $\alpha$  differs from unity at the  $\approx 2.3\sigma$  level, which is interesting but not yet significant. We find no significant difference in the scaling relations when comparing relaxed and unrelaxed systems.

Our mean  $Y_{SZ}/Y_X$  is significantly lower than that reported from the *XMM* and *Planck* analysis of the full sample of 62 clusters ( $a = -0.032 \pm 0.028$ ). However, when we repeat the *Planck* and *XMM* analysis restricting ourselves to the same 28 systems that compose the *Chandra* subsample, we find results that are in significantly better agreement ( $a = -0.166 \pm 0.036$ ), demonstrating the original tension is driven by the remaining 34 (mostly  $z \geq 0.1$ ) clusters in the full *Planck* and *XMM* cluster sample.

Compared with the *XMM-Newton* analysis, we find a significantly lower scatter in the  $Y_{SZ} - Y_X$  relation,  $\sigma_{sz|x} = 0.083 \pm 0.021$  for the *Chandra-Planck* data, versus  $\sigma_{sz|x} = 0.182 \pm 0.025$  for the full *XMM-Planck* sample. The scatter for the full *XMM-Planck* sample is at least partly driven by the systematic differences between the *Chandra* sub-sample of galaxy clusters, and the remaining systems. The *XMM-Planck* scatter for the *Chandra* subsample is lower  $\sigma_{sz|x} = 0.132 \pm 0.036$  and consistent with the scatter estimated from *Chandra* data. Finally, we note the *Chandra* data is fully consistent with no intrinsic scatter in the  $Y_{SZ}-Y_X$  relation: our central values are prior-driven.

Both the *Chandra* and *XMM* values of  $Y_{SZ}/Y_X$  for  $z < 0.1$  are significantly lower than  $a = -0.075$  expected from the observed cluster temperature profiles along (§ 2). We believe that a significant fraction of that difference can be attributed to some level of gas clumping, with  $Q \simeq 1.05$  including substructure masking (Nagai et al. 2007). Any remaining difference is within the range of current absolute accuracy of the X-ray temperature measurements and systematic uncertainty in the clumping factor correction.

In summary, we find that the observed  $Y_X - Y_{SZ}$  relation from the joint *Planck* and *Chandra* analysis is in good agreement with the theoretical expectations — it shows very low intrinsic scatter, a slope close to unity, and the amplitude is consistent with physically plausible levels of gas clumping.

In conjunction with the work in Vikhlinin et al. (2009),

our results can be used to self-consistently estimate the multi-variate scaling relation of galaxy clusters. In an upcoming work, we use these results to study the  $L_X-M$  and  $Y_{SZ}-M$  scaling relations of galaxy clusters as determined from X-ray data, and compare these to those derived from the optically selected maxBCG galaxy cluster catalog (Koester et al. 2007).

The authors would like to thank August Evrard, James Bartlett, and Eli Rykoff for useful discussions, and comments on draft versions of the manuscript. We also thank Monique Arnaud and Gabriel Pratt for useful criticism on an earlier draft of this work. ER is funded by NASA through the Einstein Fellowship Program, grant PF9-00068. AV is funded by NASA grant GO1-12168X and contract NAS8-39073. SM is supported by the KICP through the NSF grant PHY-0551142 and an endowment from the Kavli Foundation.

## REFERENCES

- Allen, S. W. et al. 2008, *MNRAS*, 383, 879  
 Andersson, K. et al. 2010, ArXiv e-prints: 1006.3068  
 Arnaud, M., Pointecouteau, E., & Pratt, G. W. 2007, *A&A*, 474, L37  
 Arnaud, M. et al. 2010, *A&A*, 517, A92+  
 Atrio-Barandela, F. et al. 2008, *ApJ*, 675, L57  
 Becker, M. R. & Kravtsov, A. V. 2010, ArXiv e-prints: 1011.1681  
 Benson, B. A. et al. 2011, ArXiv e-prints  
 Bielby, R. M. & Shanks, T. 2007, *MNRAS*, 382, 1196  
 Bonamente, M. et al. 2008, *ApJ*, 675, 106  
 Carlstrom, J. E. et al. 2011, *PASP*, 123, 568  
 Cavagnolo, K. W. et al. 2009, *ApJS*, 182, 12  
 Comis, B. et al. 2011, *MNRAS*, 418, 1089  
 Croston, J. H. et al. 2008, *A&A*, 487, 431  
 Diego, J. M. & Partridge, B. 2010, *MNRAS*, 402, 1179  
 Evrard, A. E. et al. 2008, *ApJ*, 672, 122  
 Fabjan, D. et al. 2011, ArXiv e-prints  
 Foley, R. J. et al. 2011, *ApJ*, 731, 86  
 Fowler, J. W. et al. 2007, *Appl. Opt.*, 46, 3444  
 Gull, S. F. & Northover, K. J. E. 1976, *Nature*, 263, 572  
 Hallman, E. J. et al. 2007, *ApJ*, 665, 911  
 Holder, G., Haiman, Z., & Mohr, J. J. 2001, *ApJ*, 560, L111  
 Jeltema, T. E. et al. 2008, *ApJ*, 681, 167  
 Kay, S. T. et al. 2011, ArXiv e-prints  
 Koester, B. et al. 2007, *ApJ*, 660, 239  
 Komatsu, E. et al. 2008, ArXiv e-prints, 803  
 Kravtsov, A. V., Vikhlinin, A., & Nagai, D. 2006, *ApJ*, 650, 128  
 Lau, E. T., Kravtsov, A. V., & Nagai, D. 2009, *ApJ*, 705, 1129  
 Lieu, R., Mittaz, J. P. D., & Zhang, S.-N. 2006, *ApJ*, 648, 176  
 Mantz, A. et al. 2010, *MNRAS*, 406, 1773  
 Marriage, T. A. et al. 2011, *ApJ*, 737, 61  
 Mathiesen, B., Evrard, A. E., & Mohr, J. J. 1999, *ApJ*, 520, L21  
 Melin, J.-B. et al. 2011, *A&A*, 525, A139+  
 Menanteau, F. et al. 2011, ArXiv e-prints: 1109.0953  
 Meneghetti, M. et al. 2010, *A&A*, 514, A93+  
 Moretti, A. et al. 2011, *A&A*, 528, A102  
 Mroczkowski, T. et al. 2009, *ApJ*, 694, 1034  
 Nagai, D. 2006, *ApJ*, 650, 538  
 Nagai, D., Vikhlinin, A., & Kravtsov, A. V. 2007, *ApJ*, 655, 98  
 Piffaretti, R. & Valdarnini, R. 2008, *A&A*, 491, 71  
 Planck Collaboration. 2011a, ArXiv e-prints: 1101.2026  
 —. 2011b, ArXiv e-prints: 1101.2025  
 —. 2011c, ArXiv e-prints: 1101.2043  
 —. 2011d, ArXiv e-prints: 1101.2024  
 —. 2011e, ArXiv e-prints: 1101.2022  
 —. 2011f, ArXiv e-prints  
 Pratt, G. W. et al. 2007, *A&A*, 461, 71  
 —. 2009, *A&A*, 498, 361  
 Rasia, E. et al. 2012, ArXiv e-prints  
 Rozo, E. et al. 2011, In preparation  
 Sehgal, N. et al. 2011, *ApJ*, 732, 44  
 Sifon, C. et al. 2012, ArXiv e-prints  
 Stanek, R. et al. 2010, *ApJ*, 715, 1508  
 Sun, M. et al. 2009, *ApJ*, 693, 1142  
 Sunyaev, R. A. & Zeldovich, Y. B. 1972, *Comments on Astrophysics and Space Physics*, 4, 173  
 Vanderlinde, K. et al. 2010, *ApJ*, 722, 1180  
 Vikhlinin, A. et al. 2005, *ApJ*, 628, 655  
 —. 2006, *ApJ*, 640, 691  
 —. 2009, *ApJ*, 692, 1033  
 Zwart, J. T. L. et al. 2011, *MNRAS*, 418, 2754

## APPENDIX

### CLUSTER DATA

We summarize the data employed in our analysis in table 1.

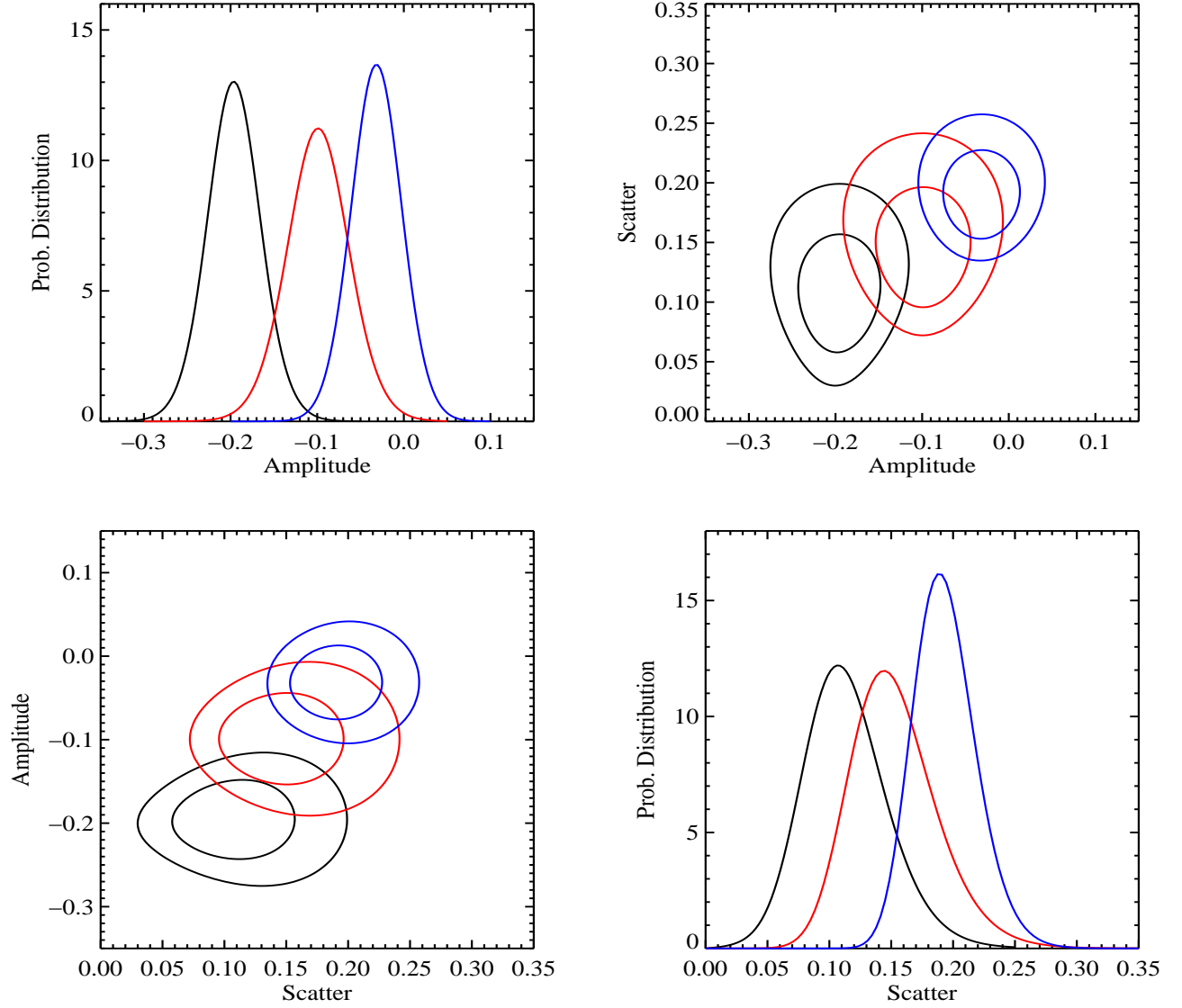


FIG. 6.— Best-fit parameters for the  $Y_{SZ}-Y_X$  scaling relation assuming a slope of unity. Black curves are obtained using *Chandra* data and the cluster sample in Table 1. Red and blue curves are using the Planck Collaboration (2011a) data. The red curves show the results when we restrict our analysis of the Planck Collaboration (2011a) data to the same galaxy clusters that constitute our *Chandra* sample. The blue curves include all galaxy clusters in Planck Collaboration (2011a). All confidence regions are 68% and 95% likelihood contours respectively.

TABLE 1  
 CLUSTER DATA

Name	P11 Redshift	Redshift	$D_A^2 Y_{SZ}$	$CY_X$ ( <i>Chandra</i> )	$CY_X$ ( <i>XMM</i> )	Merger?
A85	0.052	0.0557	$5.05 \pm 0.54$	$6.19 \pm 0.16$	$5.37 \pm 0.22$	—
A119	0.044	0.0445	$2.60 \pm 0.29$	$3.55 \pm 0.13$	$3.42 \pm 0.16$	✓
A401	0.075	0.0743	$7.71 \pm 0.74$	$10.86 \pm 0.47$	$10.42 \pm 0.75$	—
A3112	0.070	0.0759	$1.98 \pm 0.33$	$3.38 \pm 0.21$	$2.82 \pm 0.11$	—
A3158	0.060	0.0583	$3.14 \pm 0.27$	$3.10 \pm 0.07$	$3.73 \pm 0.15$	—
A478	0.088	0.0881	$8.71 \pm 0.76$	$10.17 \pm 0.58$	$9.59 \pm 0.39$	—
A3266	0.059	0.0602	$8.84 \pm 0.69$	$11.89 \pm 0.29$	$10.07 \pm 0.36$	✓
A3376	0.045	0.0455	$0.97 \pm 0.19$	$1.64 \pm 0.24$	$1.34 \pm 0.06$	✓
A1413	0.143	0.1429	$6.99 \pm 0.76$	$7.83 \pm 0.48$	$7.58 \pm 0.12$	—
ZwCl11215	0.077	0.0767	$4.32 \pm 0.66$	$5.54 \pm 0.21$	$5.72 \pm 0.30$	—
A3528s	0.053	0.0574	$2.41 \pm 0.33$	$2.00 \pm 0.15$	$1.62 \pm 0.10$	—
A1644	0.047	0.0475	$2.41 \pm 0.39$	$3.08 \pm 0.30$	$2.80 \pm 0.13$	✓
A1650	0.084	0.0823	$4.00 \pm 0.55$	$3.62 \pm 0.15$	$3.67 \pm 0.08$	—
A1651	0.084	0.0853	$3.50 \pm 0.58$	$5.32 \pm 0.29$	$4.12 \pm 0.12$	—
A1689	0.183	0.1828	$12.93 \pm 1.42$	$13.42 \pm 0.71$	$12.41 \pm 0.22$	—
A3558	0.047	0.0469	$3.95 \pm 0.47$	$4.04 \pm 0.36$	$4.50 \pm 0.18$	✓
A1795	0.062	0.0622	$4.37 \pm 0.38$	$5.34 \pm 0.18$	$6.78 \pm 0.28$	—
A1914	0.171	0.1712	$9.47 \pm 0.85$	$13.29 \pm 0.68$	$12.43 \pm 0.31$	—
A2034	0.151	0.1130	$4.27 \pm 0.58$	$5.11 \pm 0.15$	$6.01 \pm 0.14$	—
A2029	0.078	0.0779	$7.65 \pm 0.66$	$11.48 \pm 0.53$	$12.13 \pm 0.65$	—
A2065	0.072	0.0723	$3.72 \pm 0.48$	$4.35 \pm 0.16$	$4.52 \pm 0.23$	✓
A2163	0.203	0.2030	$43.01 \pm 1.99$	$60.93 \pm 3.21$	$59.75 \pm 2.14$	✓
A2204	0.152	0.1511	$10.39 \pm 0.94$	$12.96 \pm 1.00$	$11.88 \pm 0.39$	—
A2256	0.058	0.0581	$6.73 \pm 0.38$	$8.94 \pm 0.43$	$7.02 \pm 0.33$	✓
A2255	0.081	0.0800	$4.81 \pm 0.37$	$4.97 \pm 0.14$	$4.81 \pm 0.15$	—
RX J1720	0.164	0.1593	$5.68 \pm 0.72$	$6.45 \pm 0.38$	$5.69 \pm 0.14$	—
A2390	0.231	0.2302	$15.61 \pm 1.22$	$19.49 \pm 1.56$	$19.26 \pm 0.58$	—
A3921	0.094	0.0941	$3.41 \pm 0.28$	$3.75 \pm 0.15$	$3.10 \pm 0.08$	—

NOTE. — The units for  $D_A^2 Y_{SZ}$  and  $CY_X$  are  $10^{-5}$  Mpc<sup>2</sup>. The  $Y_X$  values from *XMM* are drawn from Planck Collaboration (2011a). In addition, both the  $Y_{SZ}$  and  $Y_X$  data of Planck Collaboration (2011a) are corrected to our fiducial cosmology ( $h = 0.72$ ) and to our cluster redshifts. The P11 redshift column quotes the redshifts as they appear in Planck Collaboration (2011a).